

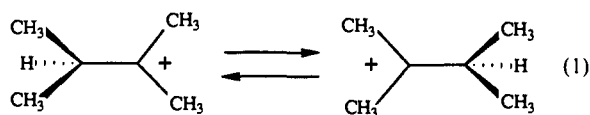
Experimental and Theoretical Studies of Nonadditivity of Multiple Isotopic Substitution on Equilibria

Martin Saunders* and Gary W. Cline

Contribution from the Department of Chemistry, Yale University, New Haven, Connecticut 06511. Received March 14, 1989

Abstract: From ^{13}C NMR spectra of mixtures of a multiply deuterium and ^{13}C substituted 2,3-dimethyl-2-butyl cation in $\text{SbF}_5/\text{SO}_2\text{ClF}$, the relative equilibrium isotope effects on the degenerate 1,2 hydride shifts were measured with very high accuracy over a range of temperatures. These isotope effects were calculated theoretically first with ab initio quantum mechanical methods to obtain the structure and the Cartesian force constant matrix and then with the Bigeleisen–Wolfsberg method for obtaining the reduced isotopic partition function ratios. The experimental and theoretical equilibrium isotope effects are in good agreement and are essentially additive for multiple ^{13}C substitution in this system; however, multiple deuterium substitution leads to strongly nonadditive results. With use of the experimental equilibrium isotope effects for the monodeuteriomethyl-, the dideuteriomethyl-, and the trideuteriomethyl-substituted ions, all of the isotope effects for the other isotopomers can be closely reproduced by assuming additivity by group. Through analysis of the theoretical results, nonadditivity of the deuterium equilibrium isotope effect within each methyl group was shown to be largely due to isotopic conformational preference.

Stable solutions of carbocations undergoing rearrangement reactions are ideal systems for the study of equilibrium isotope effects¹ by NMR spectroscopy.^{2,3} In cases where very rapid degenerate rearrangements occur, the observed NMR chemical shift of a nucleus moving among different positions is the average of the chemical shifts that the nucleus would have at each site if the process could be "frozen out", weighted by the concentrations of the equilibrating species. If the equilibrium is perturbed by the unsymmetrical introduction of one or more isotopic atoms, these concentrations are a function of the equilibrium isotope effects. The NMR frequencies can yield accurate and precise values for the equilibrium isotope effects. In particular, the rapid degenerate 1,2 hydride shifts in 2,3-dimethyl-2-butyl cation (eq 1) are evident from the ^{13}C NMR spectrum that consists of two



peaks at 198 ppm for the central carbons, the average of the expected methine and cationic carbon positions, and 32 ppm for the methyl groups interchanging between positions on and adjacent to the cationic carbon. Appropriate introduction of ^{13}C or deuterium into the cation to break the symmetry perturbs the normally degenerate equilibrium so that K_{eq} is no longer unity. This produces temperature-dependent splittings in the averaged ^{13}C NMR peaks, corresponding to the interchanging nuclei. Because of the large chemical shift differences between the interchanging sites and the narrow line widths, measurement of the ^{13}C shifts of these peaks provides an accuracy not obtained by other experimental techniques for determining the equilibrium isotope effects.

The quantitative effects of multiple isotopic substitution have

been of interest for some time. The assumption, known as "the rule of the geometric mean",^{4,5} is often invoked in the evaluation of experimentally determined kinetic and equilibrium isotope effects. It assumes that multiple isotopic substitution produces additive changes in the energy; thus, an isotope effect for multiple substitution on formally identical positions should be the product of the effects associated with individual substitutions. For example, the equilibrium or kinetic isotope effect expected for a trideuteriomethyl group might be expected to be the cube of that for a monodeuteriomethyl group. Deviations from additivity for kinetic⁶ and equilibrium^{2b} secondary β -deuterium isotope effects have been noted.

Earlier studies, which made use of ^1H NMR to observe the normally degenerate hydride shift in the 2,3-dimethyl-2-butyl cation, have produced preliminary results indicating nonadditivity on multiple deuterium isotopic substitution.^{2b} We have now reexamined this system with the substantially increased resolution of high-field ^{13}C NMR spectroscopy. We have generated mixtures of a number of polydeuterated isotopomers of this cation by using mixtures of partially deuterated starting materials in synthesizing the precursors. In order to obtain spectra with adequate signal-to-noise in reasonable data acquisition times, we prepared cation samples from polydeuterated isotopomers of 2,3-dimethyl-2-butanol 90% enriched with ^{13}C at the hydroxyl carbon. The ^{13}C NMR peaks of the d_1 – d_5 isotopomers have been resolved and assigned to specific species and the shifts measured. A great advantage of doing the experiment this way is that all of the isotopomers are observed at the same time and in the same environment; thus, all external factors affecting the equilibrium isotope effects are identical, and the relative isotope effects are, therefore, measured with very great accuracy.

We have also generated mixtures of all possible dilabeled ^{13}C isotopomers of the 2,3-dimethyl-2-butyl cation. The mixtures consist of isotopomers for which the equilibrium of the hydride shift is perturbed by primary and combinations of primary and secondary ^{13}C isotope effects. As in the deuterium case, following assignment of the peaks to specific isotopomers, we could then obtain accurate ^{13}C isotope effects. The precise experimental data for the equilibrium isotope effects in the array of isotopomers provide an excellent opportunity for comparison with theoretical predictions.

(1) For general treatments of isotope effects, see: (a) Bigeleisen, J.; Wolfsberg, M. *Adv. Chem. Phys.* **1958**, *1*, 15. (b) Melander, L. *Isotope Effects on Reaction Rates*; Ronald Press: New York, 1960. (c) Collins, C. J.; Bowman, N. S., Eds. *Isotope Effects in Chemical Reactions*; ACS Monograph 167; Van Nostrand Reinhold: New York, 1970. (d) Wolfsberg, M. *Acc. Chem. Res.* **1972**, *7*, 225. (e) Melander, L.; Saunders, W. H., Jr. *Reaction Rates of Isotopic Molecules*; Wiley: New York, 1980.

(2) (a) Saunders, M.; Jaffe, M. H.; Vogel, P. *J. Am. Chem. Soc.* **1971**, *93*, 2558. (b) Saunders, M.; Vogel, P. *J. Am. Chem. Soc.* **1971**, *93*, 2561. (c) Saunders, M.; Vogel, P.; Hagen, E. L.; Rosenfeld, J. *J. Acc. Chem. Res.* **1973**, *6*, 53. (d) Saunders, M.; Kates, M. R. *J. Am. Chem. Soc.* **1978**, *100*, 7082. (e) Saunders, M.; Kates, M. R.; Walker, G. E. *J. Am. Chem. Soc.* **1981**, *103*, 4623.

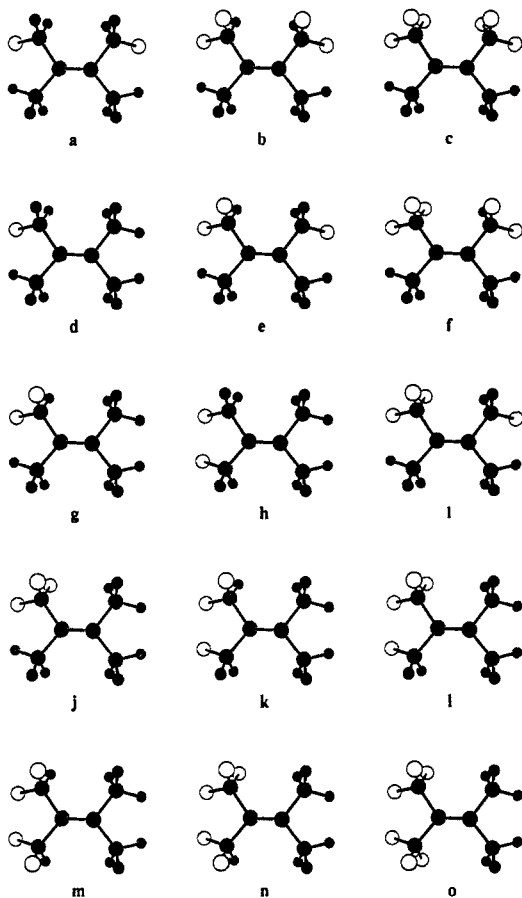
(3) For a general review: Siehl, H.-U. In *Advances in Physical Organic Chemistry*; Bethell, D., Ed.; Academic Press: London, 1987; Vol. 23, pp 63–163.

(4) Bigeleisen, J. *J. Chem. Phys.* **1955**, *23*, 2264.

(5) Gold, V. In *Advances in Physical Organic Chemistry*; Gold, V., Ed.; Academic Press: London, 1969; Vol. 7, pp 266–267.

(6) Shiner, V. J., Jr.; Murr, B. L.; Heinemann, G. *J. Am. Chem. Soc.* **1963**, *85*, 2413.

Chart I

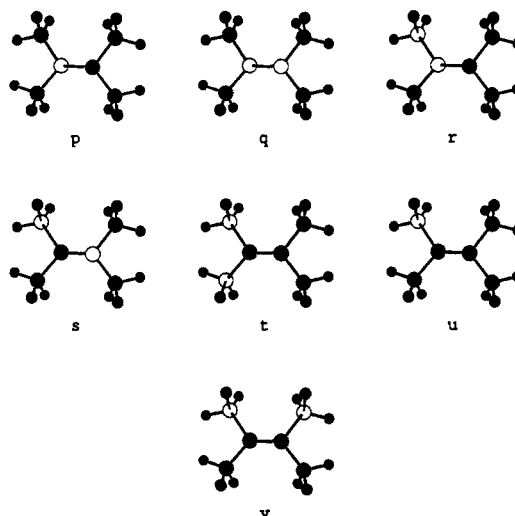


Theoretical Evaluation of Equilibrium Isotope Effects

In order to calculate theoretical values for the equilibrium isotope effects for the 2,3-dimethyl-2-butyl cation, we required the minimum energy geometry and the Cartesian force constant matrix (the second derivatives of the energy in Cartesian coordinates). We obtained these by means of ab initio quantum mechanical calculations⁷ using the GAUSSIAN 86 molecular orbital program.⁸ Within the framework of the Born-Oppenheimer approximation, they are independent of isotopic substitution. Geometry optimization was carried out at the 3-21G and 6-31G* levels, and the analytical Cartesian force constant matrix was obtained at the 3-21G level. It is striking that the lowest energy (classical) structures found in both calculations have no symmetry. We might have also examined the hydrido-bridged nonclassical cation. However, for the purposes of this paper, that was not necessary. The symmetrical, nonclassical structure for this ion has been ruled out for the stable ion by the very observation of the ¹³C and deuterium equilibrium isotope effects that we consider in this paper. The barrier for the hydride shift, which must go via this nonclassical ion, was found to be 3.4 kcal/mol from examination of the ¹³C NMR line shape at very low temperatures.^{2d}

Equilibrium isotope effects on the, normally degenerate, 1,2 hydride shift were calculated with the program QUIVER.⁹ It uses the standard output of the Cartesian force constant matrix from the GAUSSIAN 82 or 86 molecular orbital program package as input to calculate the vibrational frequencies for the desired isotopomers

Chart II



and, from them, the reduced isotopic partition function ratios, $(s_2/s_1)f$.^{1d,10}

Since the structure for the ion has no symmetry, all possible arrangements (conformations) of the isotope are required to calculate equilibrium isotope effects.¹¹ Rotation around all of the single bonds is rapid on the NMR time scale, so that a single averaged pair of lines is observed for all the interconverting conformers for each isotopomer. For example, the isotopomer with a single deuterium on a methyl group (1d, Chart I) requires one to consider the six different structures with deuterium substituted on the methyl groups attached to the cation center and six more with deuterium on the methyl groups away from the cation center. Since we are using ¹³C NMR spectroscopy to accurately measure the deuterium isotope effects, all the molecules we observe *must* also have ¹³C. Unless we prepared ions (1q, Chart II)^{2e} where the central carbons are both ¹³C, the ions we examine, containing a single ¹³C, are also affected by a ¹³C equilibrium isotope effect. In the monolabeled ¹³C ion, a total of 24 structures must therefore be considered for the simple case of a single deuterium on a methyl group. The $(s_2/s_1)f$'s for all these conformers are referenced to the isotopically light molecule. The equilibrium isotope effect can then be calculated by taking the sum of the $(s_2/s_1)f$'s for the set of structures where deuterium is in methyl groups attached to the methine carbon divided by the sum of the $(s_2/s_1)f$'s for the structures where it is on the opposite side. The theoretically predicted population for any single conformation can be obtained by dividing its $(s_2/s_1)f$ by the sum of the $(s_2/s_1)f$'s for all equilibrating conformers. It turned out, however, that all the ¹³C NMR peaks were shifted the same amount in the same direction by the ¹³C equilibrium isotope effect. Thus, in the QUIVER calculations on the mono- and dilabeled ¹³C species, the calculated splittings in the ¹³C NMR spectrum are almost exactly the same. Any differences would be due to non-additivity of deuterium, and ¹³C effects and are evidently too small to see.

Theoretical Results on the Structure of the Cation

The deviations from symmetry in the structure found in the theoretical study are informative. The 3-21G and 6-31G* optimized structures (Figure 1; Table I) are suggestive of a geometry strongly affected by hyperconjugation.^{6,12} The discussion of the

(7) Hehre, W. J.; Radom, L.; Schleyer, P. v. R.; Pople, J. A. *Ab Initio Molecular Orbital Theory*; Wiley-Interscience: New York, 1986.

(8) Frisch, M. J.; Binkley, J. S.; Schlegel, H. B.; Raghavachari, K.; Melius, C. F.; Martin, R. L.; Stewart, J. J. P.; Bobrowicz, F. W.; Rohlfing, C. M.; Kahn, L. R.; DeFrees, D. J.; Seeger, R.; Whiteside, R. A.; Fox, D. J.; Fluder, E. M.; Pople, J. A. GAUSSIAN 86; Carnegie-Mellon Quantum Chemistry Publishing Unit: Pittsburgh, PA, 1984.

(9) Saunders, M.; Laidig, K. E.; Wolfsberg, M. *J. Am. Chem. Soc.* **1989**, *111*, 8989.

(10) Bigeleisen, J.; Mayer, M. G. *J. Chem. Phys.* **1947**, *15*, 261.

(11) Saunders, M.; Cline, G. W.; Wolfsberg, M. *Z. Naturforsch., A: Phys., Phys. Chem., Kosmophys.* **1989**, *44a*, 480.

(12) (a) Sunko, D. E.; Szele, I.; Hehre, W. J. *J. Am. Chem. Soc.* **1977**, *99*, 5000. (b) DeFrees, D. J.; Hehre, W. J.; Sunko, D. E. *J. Am. Chem. Soc.* **1979**, *101*, 2323. (c) DeFrees, D. J.; Taagepera, M.; Levi, B. A.; Pollack, S. K.; Summerhays, K. D.; Taft, R. W.; Wolfsberg, M.; Hehre, W. J. *J. Am. Chem. Soc.* **1979**, *101*, 5532. (d) Hehre, W. J.; Hout, R. F., Jr.; Levi, B. A. *J. Comput. Chem.* **1983**, *4*, 499.

Table I. Ab initio Optimized Geometry^a of the 2,3-Dimethyl-2-butyl Cation

		Z Matrix (+11) ^b					
1	C	6	C 1 D5 2 A4 3 T3	11	H 4 D10 2 A9 1 T8	16	H 5 D15 1 A14 2 T13
2	C 1 D1	7	H 2 D6 1 A5 3 T4	12	H 4 D11 2 A10 1 T9	17	H 6 D16 1 A15 2 T14
3	C 2 D2 1 A1	8	H 3 D7 2 A6 1 T5	13	H 4 D12 2 A11 1 T10	18	H 6 D17 1 A16 2 T15
4	C 2 D3 1 A2 3 T1	9	H 3 D8 2 A7 1 T6	14	H 5 D13 1 A12 2 T11	19	H 6 D18 1 A17 2 T16
5	C 1 D4 2 A3 3 T2	10	H 3 D9 2 A8 1 T7	15	H 5 D14 1 A13 2 T12		

Optimized Parameters ^c					
D1	1.4760 (1.4681)	A1	103.3202 (102.4156)	T1	122.5254 (119.9187)
D2	1.5696 (1.5939)	A2	116.3148 (116.2157)	T2	87.3227 (86.2067)
D3	1.5318 (1.5379)	A3	119.6850 (119.8616)	T3	266.7501 (266.9610)
D4	1.4758 (1.4783)	A4	121.4950 (121.3609)	T4	247.0297 (246.9220)
D5	1.4768 (1.4783)	A5	108.0343 (109.476)	T5	66.5048 (65.0889)
D6	1.0845 (1.0827)	A6	111.5273 (110.7695)	T6	184.5853 (182.9664)
D7	1.0828 (1.0812)	A7	106.7341 (106.1378)	T7	303.0614 (301.4984)
D8	1.0820 (1.0816)	A8	112.8041 (112.3775)	T8	58.9792 (59.8708)
D9	1.0828 (1.0812)	A9	111.7229 (111.6166)	T9	177.3900 (178.3318)
D10	1.0840 (1.0833)	A10	108.5461 (108.4775)	T10	296.3186 (297.1235)
D11	1.0824 (1.0822)	A11	112.4467 (111.9745)	T11	-11.2693 (-9.9653)
D12	1.0830 (1.0820)	A12	113.3367 (113.3365)	T12	106.7828 (113.5660)
D13	1.0799 (1.0788)	A13	105.0834 (106.7364)	T13	221.7511 (228.4686)
D14	1.0941 (1.0942)	A14	111.7569 (110.9385)	T14	36.5204 (38.8560)
D15	1.0834 (1.0856)	A15	111.8389 (111.5933)	T15	162.7503 (164.3733)
D16	1.0827 (1.0836)	A16	113.0597 (113.0081)	T16	281.4116 (283.6612)
D17	1.0798 (1.0791)	A17	105.7005 (106.7670)		
D18	1.0928 (1.0937)				

Interatomic Angles ^c			
C1-C2-C3	103.3202 (102.4156)	C1-C2-C4	116.3148 (116.2157)
C3-C2-C4	111.5219 (110.0002)	C2-C1-C5	119.6850 (119.8616)
C2-C1-C6	121.4950 (121.3609)	C5-C1-C6	118.8175 (118.7732)
C1-C2-H7	108.0343 (109.5476)	C3-C2-H7	106.8443 (106.7870)
C4-C2-H7	110.2172 (111.1631)	C2-C3-H8	111.5273 (110.7695)
C2-C3-H9	106.7341 (106.1378)	H8-C3-H9	108.2811 (108.7481)
C2-C3-H10	112.8041 (112.3775)	H8-C3-H10	109.2916 (110.0807)
H9-C3-H10	108.0179 (108.5697)	C2-H4-H11	111.7229 (111.6166)
C2-C4-H12	108.5461 (108.4775)	H11-C4-H12	107.5372 (107.6648)
C2-C4-H13	112.4467 (111.9745)	H11-C4-H13	108.7860 (109.1781)
H12-C4-H13	107.6023 (107.7592)	C1-C5-H14	113.3367 (113.3365)
C1-C5-H15	105.0834 (106.7364)	H14-C5-H15	108.2909 (108.6226)
C1-C6-H17	111.8389 (111.5933)	C1-C6-H18	113.0597 (113.0081)
H17-C6-H18	111.0429 (110.6932)	C1-C6-H19	105.7005 (106.7670)
H17-C6-H19	106.1721 (105.8326)	H18-C6-H19	108.5931 (108.5651)

^aOptimized by the GAUSSIAN 86 molecular orbital program at the 6-31G* (3-21G) level. ^bAtom numbers are those shown in Figure 1. ^cUnits for bond lengths, D_n, are angstroms; bond angles, A_n, and torsion angles, T_n, are degrees.

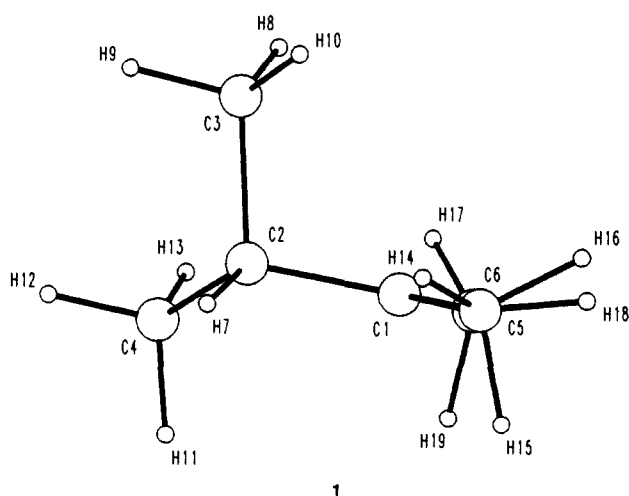


Figure 1. Ab initio optimized structure (6-31G*) of the 2,3-dimethyl-2-butyl cation (1).

structure refers to the numbering of atoms in Figure 1 to identify specific bonds, bond lengths, bond angles, and torsion angles. The C-H bonds on methyls attached to C* show striking differences in bond lengths, as the torsion angle with respect to the vacant p-orbital changes. At 6-31G*, two C-H bonds have torsion angles allowing substantial overlap with the vacant p-orbital, 16.8° for C₅-H₁₅ and 11.4° for C₆-H₁₉ (23.6° and 13.7° at 3-21G). They have bond lengths that are significantly longer, 1.0941 and 1.0928

Å (1.0942 and 1.0937 Å at 3-21G), respectively, than for C-H bonds orthogonal to the vacant p-orbital, 1.0798 Å for C₅-H₁₄ and 1.0799 Å for C₆-H₁₈ (1.0788 and 1.0791 Å at 3-21G), which have torsion angles of 78.7° and 72.8°, respectively (82.0° and 74.4° at 3-21G). If the force constant varies in the normal manner with bond length, these results imply that deuterium should be disfavored at positions 15 and 19 and favored at 14 and 18.

Associated with the lengthening of C-H bonds is a change of bond angles. The smallest H-C-H bond angles in the methyl groups next to the cationic carbon are between those C-H bonds that show maximum vacant p-orbital overlap and those C-H bonds midway between orthogonal and overlapping; thus, H₁₅-C₅-H₁₆ and H₁₇-C₆-H₁₉ have bond angles of 106.4° and 106.2°, respectively (105.9° and 105.8° at 3-21G). The largest H-C-H bond angles are associated with the orthogonal C-H bonds and with those C-H bonds midway between orthogonal and overlapping; thus, H₁₄-C₅-H₁₆ and H₁₇-C₆-H₁₈ have bond angles of 111.5° and 111.0°, respectively (110.9° and 110.7° at 3-21G). Analogous effects are seen for the C-C-H bond angles where the longer bonds are associated with smaller bond angles, C₁-C₅-H₁₅ and C₁-C₆-H₁₉ have bond angles of 105.1° and 105.7°, respectively (106.7° and 106.8° at 3-21G), and shorter bonds dictate greater bond angles, C₁-C₅-H₁₄ and C₁-C₆-H₁₈ have bond angles of 113.3° and 113.1°, respectively (113.3° and 113.0° at 3-21G). The geometry of the methyl groups next to the cationic carbon suggests a large deuterium isotope effect due to C-H(D) hyperconjugation partially offset by an inverse deuterium isotope effect for conformations in which the C-H(D) bond is close to orthogonal to the vacant p-orbital.

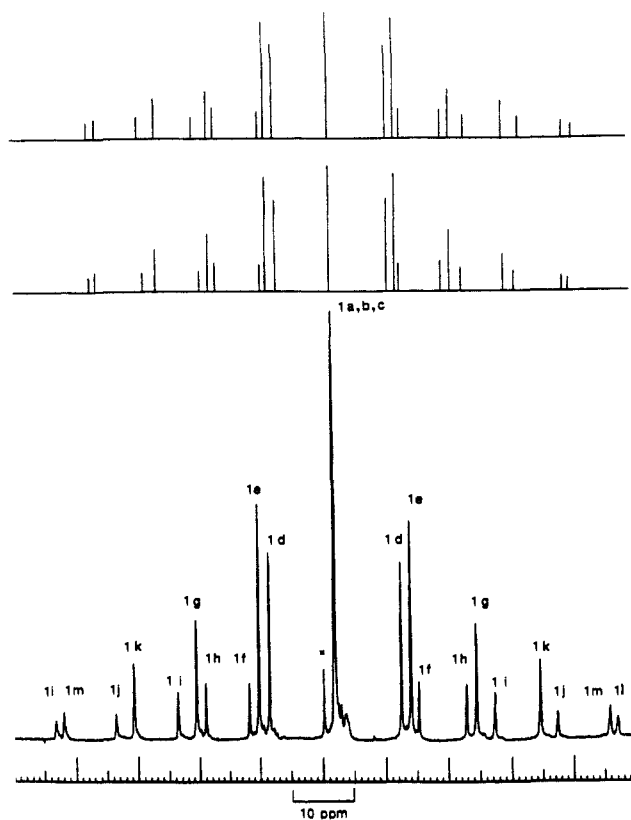


Figure 2. Lower trace: proton-decoupled ^{13}C NMR spectra, centered at $\delta \sim 200$, of averaged cation/methine C resonances of ^2H isotopomers of the 2,3-dimethyl-2-butyl cation in $\text{SbF}_5/\text{SO}_2\text{ClF}$ at -100°C . Peak assignments are isotopomers of Chart 1. Unidentified peak, \times . Middle trace: spectra predicted by QUIVER. Upper trace: spectra predicted assuming nonadditive isotope effects arise only from nonstatistical distribution of isotopic conformers.

The structure of the isopropyl group also shows significant effects due to C–C hyperconjugation. In the theoretical structure, one of the C–C bonds, $\text{C}_2\text{--C}_3$, is almost parallel to the vacant p-orbital. As in the case of hyperconjugative interaction of C–H bonds with the cationic carbon, a significant increase in bond length, 1.5696 Å for $\text{C}_2\text{--C}_3$ vs 1.5318 Å for $\text{C}_2\text{--C}_4$ at 6-31G* (1.5939 vs 1.5379 Å at 3-21G), is evident. The associated decrease in C–C–C bond angle is also clear for C_2 compared to C_3 . The $\text{C}_1\text{--C}_2\text{--C}_3$ bond angle of 103.3° (102.4° at 3-21G) is significantly less than that of the $\text{C}_1\text{--C}_2\text{--C}_4$ bond angle of 116.3° (116.2° at 3-21G).

The hyperconjugative lengthening of one C–C bond of the isopropyl is associated with minor differences in the C–H bonding patterns of the methyls. Noted are (1) a decrease of average C–C–H bond angles, 110.3° for $\text{C}_2\text{--C}_3\text{--H}$ vs 110.9° for $\text{C}_2\text{--C}_4\text{--H}$ (108.6° vs 110.7° at 3-21G), and (2) a minor shortening of the C–H methyl bonds, 1.0825 Å for $\text{C}_3\text{--H}$ vs 1.0831 Å for $\text{C}_4\text{--H}$ (1.0813 vs 1.0825 Å at 3-21G), and increase of the average H–C–H bond angles, 108.5° for H– $\text{C}_3\text{--H}$ vs 108.0° for H– $\text{C}_4\text{--H}$ (109.1° vs 108.2° at 3-21G). One might, therefore, expect very little conformational preference between different conformers with deuterium on methyls away from the cationic carbon. However, C–C hyperconjugation should contribute to a carbon isotope effect (secondary) in which ^{13}C is disfavored on the methyl away from the cationic center with its C–C bond parallel to the p-orbital.

Experimental Deuterium Equilibrium Isotope Effects

Figure 2 (lower trace) is a representative ^{13}C NMR spectrum of the mixture of deuterium isotopomers of the 2,3-dimethyl-2-butyl cation with deuteration restricted to no more than two methyl groups. Migration of deuterium from its original methyl group requires extensive isomerization through the other two isomeric tertiary hexyl cations,^{2a} the extent of which is easily monitored

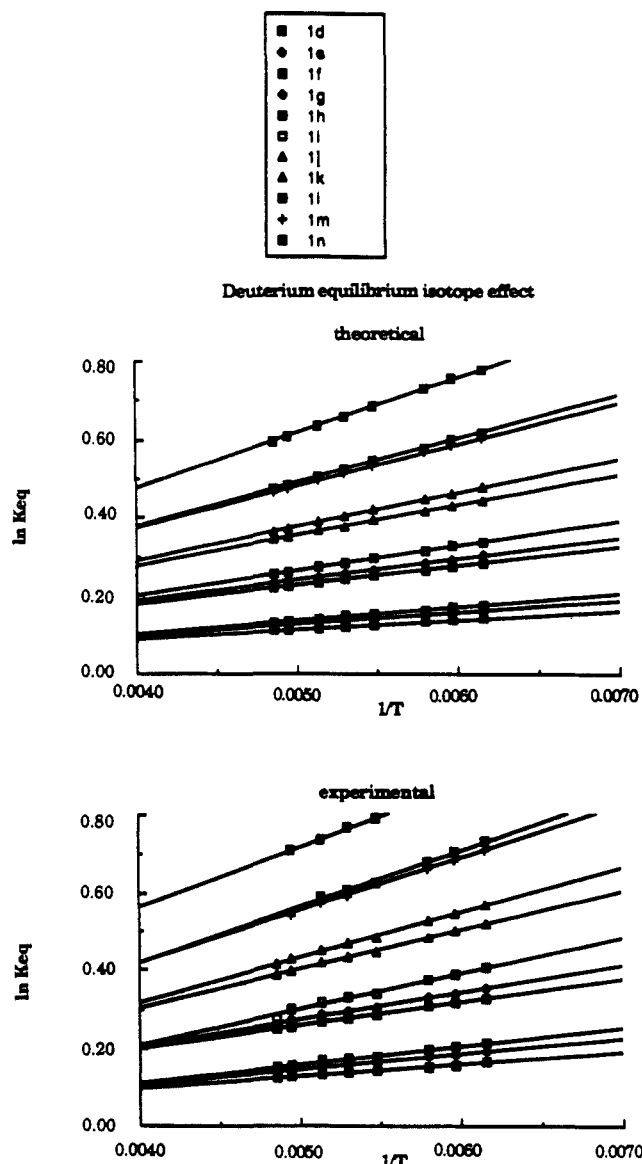


Figure 3. Lower plot: experimentally determined deuterium equilibrium isotope effects for hydride shift of the 2,3-dimethyl-2-butyl cation. Upper plot: theoretically determined deuterium equilibrium isotope effects for the hydride shift of the 2,3-dimethyl-2-butyl cation.

by following the appearance of peaks corresponding to the other isomers¹³ and was found not to occur under the experimental conditions of cation preparation and observation. In order to make peak assignments, a sample was prepared from a precursor that was labeled on a single methyl group. The three sets of peaks obtained could be assigned to the isotopomers with one, two, and three deuteriums on a single methyl group. Cations prepared from a sample of the precursor where two methyl groups were randomly labeled had many more peaks. The three sets of peaks previously seen could readily be identified, and this assignment was checked by examining cations made from a mixture of the two precursors. The other peaks were assigned by an analysis of the observed equilibrium isotope effects for the isotopomers with substitution within a single methyl group and by comparison with the values determined by theoretically calculated equilibrium isotope effects.

For the cation mixture, partially deuterated on two methyl groups, rapid 1,2 methide and hydride shifts and rapid rotation around single bonds produce an equilibrium mixture of 15 deuterium isotopomers. The isotopomers can be grouped into seven categories (Chart I). Group I consists of three isotopomers, 1a–c, which are expected to have an equilibrium constant for the hydride

(13) Olah, G. A.; Donovan, D. J. *J. Am. Chem. Soc.* 1977, 99, 5026.

Table II. Experimental and Theoretical ^2H Equilibrium Isotope Effects for Isotopomers 1d-o^a

	K_{eq}				δ (Hz)				
	temp (K)	exptl ^b	calcd ^c		exptl ^d	calcd ^e			
One-Deuterium Excess									
1d	162.55	1.1778	1.1515	1415.383	1220.782				
	167.55	1.1712	1.1466	1367.119	1183.680				
	172.55	1.1656	1.1419	1325.648	1148.574				
	182.55	1.1529	1.1334	1230.877	1083.736				
	188.85	1.1485	1.1284	1198.598	1046.174				
	194.85	1.1439	1.1241	1163.531	1012.504				
	202.25	1.1364	1.1190	1106.527	973.542				
	206.05	1.1321	1.1165	1073.740	954.548				
	ΔH^f	58.9 \pm 1.3	47.4						
	Three-Deuteriums Excess								
1j	162.55	1.7664	1.6117	4802.619	4060.324				
	167.55	1.7274	1.5858	4623.538	3927.588				
	172.55	1.6945	1.5619	4468.387	3802.480				
	182.55	1.6221	1.5192	4113.205	3572.662				
	188.85	1.5992	1.4952	3996.386	3440.278				
	194.85	1.5733	1.4741	3862.274	3322.094				
	202.25	1.5348	1.4503	3657.806	3185.910				
	206.05	1.5150	1.4389	3549.672	3119.744				
	ΔH	230.0 \pm 4.7	172.7						
	$\Delta H/^2\text{H}$	76.7	57.6						
Four-Deuteriums Excess									
1k	162.55	1.6794	1.5574	4395.934	3778.566				
	167.55	1.6485	1.5356	4244.794	3661.798				
	172.55	1.6222	1.5153	4113.371	3551.364				
	182.55	1.5635	1.4786	3810.816	3347.536				
	188.85	1.5441	1.4579	3707.716	3229.544				
	194.85	1.5242	1.4396	3600.074	3123.848				
	202.25	1.4907	1.4188	3415.320	3001.624				
	206.05	1.4737	1.4088	3319.566	2942.074				
	ΔH	195.4 \pm 4.2	152.8						
	$\Delta H/^2\text{H}$	65.1	50.9						
Two-deuterium Excess									
1g	162.55	1.4255	1.3525	3041.348	2597.822				
	167.55	1.4069	1.3393	2930.919	2514.538				
	172.55	1.3913	1.3270	2836.542	2435.996				
	182.55	1.3558	1.3046	2618.436	2291.588				
	188.85	1.3440	1.2920	2544.139	2208.314				
	194.85	1.3320	1.2807	2467.846	2133.912				
	202.25	1.3115	1.2679	2336.253	2048.096				
	206.05	1.3003	1.2618	2263.447	2006.372				
	ΔH	136.9 \pm 3.1	105.8						
	$\Delta H/^2\text{H}$	68.5	52.9						
Five-Deuterium Excess									
1h	162.55	1.3873	1.3260	2812.599	2429.408				
	167.55	1.3720	1.3146	2718.539	2356.274				
	172.55	1.3589	1.3039	2637.883	2287.016				
	182.55	1.3293	1.2845	2450.597	2158.956				
	188.85	1.3195	1.2734	2388.267	2084.682				
	194.85	1.3087	1.2635	2318.080	2018.056				
	202.25	1.2912	1.2521	2203.621	1940.902				
	206.05	1.2821	1.2467	2143.162	1903.266				
	ΔH	117.8 \pm 2.5	94.0						
	$\Delta H/^2\text{H}$	58.9	47.0						
Six-Deuteriums Excess									
1i	162.55	1.5004	1.3996	3469.493	2887.162				
	167.55	1.4753	1.3831	3328.621	2787.024				
	172.55	1.4542	1.3678	3208.470	2693.044				
	182.55	1.4075	1.3404	2934.082	2521.410				
	188.85	1.3925	1.3250	2843.929	2423.124				
	194.85	1.3760	1.3114	2743.098	2335.732				
	202.25	1.3511	1.2961	2588.711	2235.438				
	206.05	1.3208	1.2887	2396.072	2186.866				
	ΔH	181.0 \pm 8.2	125.7						
	$\Delta H/^2\text{H}$	90.5	62.9						
Four-Deuteriums Excess									
1l	162.55	2.0820	1.8558	6086.257	5195.202				
	167.55	2.0247	1.8182	5873.048	5033.202				
	172.55	1.9762	1.7835	5686.401	4879.942				
	182.55	1.8711	1.7217	5259.701	4597.000				
	188.85	1.8397	1.6872	5126.336	4433.198				
	194.85	1.8012	1.6570	4958.375	4286.470				
	202.25	1.6229	1.6229	4116.824	4116.824				
	206.05	1.6066	1.6066	4034.184	4034.184				
	ΔH	285.1 \pm 10.1	219.7						
	$\Delta H/^2\text{H}$	71.3	54.9						
Five-Deuterium Excess									
1m	162.55	2.0333	1.8293	5905.719	5081.332				
	167.55	1.9812	1.7937	5705.974	4925.256				
	172.55	1.9377	1.7608	5533.498	4777.468				
	182.55	1.8711	1.7021	5259.701	4504.252				
	188.85	1.8071	1.6691	4984.545	4345.938				
	194.85	1.7755	1.6403	4843.672	4203.962				
	202.25	1.7209	1.6076	4593.017	4039.658				
	206.05	1.5920	1.5920	3959.558	3959.558				
	ΔH	268.7 \pm 7.4	211.7						
	$\Delta H/^2\text{H}$	67.2	52.9						
Six-Deuteriums Excess									
1n	162.55	4.0970	3.2450	11386.830	9168.356				
	167.55	3.8677	3.1524	11040.540	8986.136				
	172.55	3.6701	3.0125	10714.620	8694.960				
	182.55	3.5395	2.8882	10483.760	8418.658				
	188.85	3.2791	2.7562	9981.300	8105.484				
	194.85	3.0145	2.5371	9404.150	7533.748				
	202.25	2.8791	2.4599	9078.230	7314.974				
	206.05	2.6031	2.2321	8338.120	6608.762				
	ΔH	418.9 \pm 11.3	350.7						
	$\Delta H/^2\text{H}$	69.8	58.5						
Six-Deuteriums Excess									
1o ^g	135.15	4.0970	3.2450	11386.830	9168.356				
	138.15	3.8677	3.1524	11040.540	8986.136				
	143.15	3.6701	3.0125	10714.620	8694.960				
	148.15	3.5395	2.8882	10483.760	8418.658				
	154.15	3.2791	2.7562	9981.300	8105.484				
	166.15	3.0145	2.5371	9404.150	7533.748				
	171.15	2.8791	2.4599	9078.230	7314.974				
	189.15	2.6031	2.2321	8338.120	6608.762				
	ΔH	418.9 \pm 11.3	350.7						
	$\Delta H/^2\text{H}$	69.8	58.5						

^a Refer to Chart I. ^b Evaluated as $(\Delta + \delta)/(\Delta - \delta)$, δ measured for equilibrating cation/methine carbons, $\Delta = 276$ ppm. ^c Equilibrium isotope effect calculated with QUIVER. ^d δ recorded at 62.8 MHz. ^e δ calculated at 62.8 MHz for equilibrating cation/methine carbons, $\Delta = 276$ ppm. ^f Units: cal/mol. ^g Experimental data from ref 20.

Table III. Additivity by Group

isotopomer	K_{eq}^a at 162.55 K	calcd with group additivity	source
1e	1.2106	1.2103	2/1
1f	1.2396	1.2391	3/2
1h	1.3873	1.3872	1 × 1
1i	1.5004	1.4997	3/1
1k	1.6794	1.6789	2 × 1
1m	2.0333	2.0321	2 × 2
1l	2.0820	2.0804	3 × 1
1n (at 182.55 K)	2.2025	2.1992	3 × 2

^aThe values for K_{eq} at 162.55 K (182.55 K) for **1d**, **1g**, and **1j** that were used as 1, 2, and 3 were as follows: 1.1778 (1.1529), 1.4255 (1.3558), and 1.7664 (1.6221).

shift of unity due to symmetrical deuteration. The chemical shift of the inner two carbons appears at approximately the same position as the completely nondeuterated cation, ~198 ppm. The observed splitting in this peak (0.1 ppm) is due to the intrinsic deuterium shift on ¹³C.¹⁴ Group II consists of three isotopomers, **1d–f**, with one more deuterium on one side than on the other. Group III contains three isotopomers, **1g–i**, with an excess of two deuteriums on one side. Group IV has two isotopomers, **1j** and **1k**, with an excess of three deuteriums on one side. Group V consists of two isotopomers, **1l** and **1m**, with an excess of four deuteriums on one side. Groups VI and VII are each composed of single isotopomers, **1n** and **1o**, with an excess of five and six deuteriums on one side, respectively.

Experimental and theoretical values for the equilibrium isotope effects and the chemical shift differences, δ , of the deuterium isotopomers comprising groups II–VII are contained in Table II.

Discussion of Additivity

One can examine the results for additivity, or the lack of it, in two different ways. If each deuterium on one side of the ion had the same effect on the equilibrium and every deuterium on the other side had the opposite effect, the equilibrium constant, and hence the splitting, would simply be a function of the difference between the number of deuteriums on one side and the number on the other side. The three isotopomers with one more deuterium on one side than on the other side should be expected to have the same equilibrium constant so that their ¹³C NMR peaks would coincide. The three isotopomers with a deuterium excess of two should also show the same splitting, and the same should be true for the two isotopomers with an excess of three on one side and the two with an excess of four. The spectrum (Figure 2) immediately shows that this is very far from true. Plots of $\ln K_{eq}$ vs $1/T$ (Figure 3) also demonstrate that each isotopomer, within the groups characterized as having an excess of one, two, three, and four deuteriums on one side, is quite different from the others. Multiple deuteration thus produces *very nonadditive* changes in equilibrium isotope effects here.

Another prediction of the additivity assumption is that the equilibrium isotope effect for the ion with a dideuteriomethyl group should be the square of that for the monodeuterated species and that for a trideuteriomethyl group should be its cube. At 162.5 K, the equilibrium isotope effect for the monodeuterated cation was found to be 1.1778. The value for the dideuteriomethyl ion was 1.4255 and for the trideuteriomethyl ion 1.7664. The square and cube of the monodeuterio value are 1.3872 and 1.6338, respectively, values *very far from those expected for additivity*.

However, if one gives up the idea of additivity by deuterium atoms and instead considers the possibility of additivity by group, one immediately has much better success. *One can use the equilibrium isotope effects for the simple deuteriomethyl, dideuteriomethyl, and trideuteriomethyl cations to predict all the others.* Let us call the equilibrium isotope effects for these ions at any temperature 1, 2, and 3. Then for isotopomer **1k**, for example, with a deuteriomethyl and a dideuteriomethyl group on the same side we take 2 × 1. For isotopomer **1e** with the same

groups on opposite sides we use 2/1. Table III indicates that this idea works very well indeed. We conclude that deuteriums on one methyl produce effects that are almost independent of those on another methyl. Another important conclusion from Table III is that the experimental values must have very high relative accuracy, as we expected (unless there is deviation from additivity that accidentally almost exactly cancels out experimental errors in each case).

This additivity, which is excellent when deuteriums are on different methyl groups, is very poor for deuteriums on the same methyl. Why? There are two reasons that we considered. Two deuterium atoms on the same carbon are both involved in the same vibrational motions, in particular H–C–H bending. Their effect on the frequencies of such motions could produce nonadditive changes in the isotope effect.^{12c,d,15} The second way in which nonadditivity can arise involves the conformations for rotation of the methyl group. If, as expected and indicated by the theoretical results, the hyperconjugative interaction of a C–H next to a cation is a sensitive function of the dihedral angle,^{12a,b} and if the isotope effect varies accordingly, then nonadditivity can arise from this source. A simple way of putting it is that when one deuterium occupies its most desirable position, the next one must take a different place.

We might call these two effects intrinsic nonadditivity and conformational nonadditivity (which might also be described as an isotope effect on conformation). How can we discover the relative magnitudes of these two effects? The theoretical calculations provide a means for examining this question. The asymmetric geometry of the ab initio optimized structure makes all hydrogen positions different. The probability of deuterium occupying each position on each methyl group (i.e., the equilibrium population of each individual isotopic conformer) can be predicted as the quotient of the reduced isotopic partition function ratio of each isotopic conformer divided by the sum of the reduced isotopic partition function ratios of all equilibrating conformers (Table IV, middle column). These calculations should, in principle, include *both* intrinsic and conformational effects.

If one were to assume that the nonadditivity arises from conformational preference only, i.e., that within each conformer there is additivity, then one should be able to predict the population for any isotopomer using just the theoretical $(s_2/s_1)f'$'s for the conformations of the monodeuterated isotopomer. One should be able to simply multiply together the $(s_2/s_1)f'$'s for monosubstitution at all the different sites where isotopic substitution in a conformer has occurred to obtain the equivalent of the $(s_2/s_1)f'$'s for multisubstitution. On normalizing the set of these composite $(s_2/s_1)f'$'s, one would obtain a set of predicted conformational populations for the multisubstituted species (Table IV, last column). These can be compared with the $(s_2/s_1)f'$'s obtained through the complete theoretical treatment of multisubstitution (and also with the experimental values).

The contributions of conformationally dependent and independent sources of nonadditive equilibrium isotope effects can be evaluated by examining the effect of increasing deuteration on a single methyl group compared with the effect of placing deuterium in a remote methyl group (Table IV). The two methods of predicting the equilibrium isotope effect are in very close agreement for isotopomer **1h**, indicating little perturbation of vibrational modes in one methyl group as the result of isotopic substitution in a remote methyl group. When one has several deuteriums on one methyl group, there are small differences. For isotopomers **1g** and **1j**, the assumption that conformational preference is the source of nonadditive equilibrium isotope effects leads to a larger equilibrium isotope effect than that provided by the full theoretical treatment. The difference is probably due to intrinsic nonadditivity (the cooperative effect of multiple deuteration on vibrational frequencies). However, the quite similar magnitudes of equilibrium isotope effects predicted by the two methods (Figure 2, middle and upper spectra¹⁶) indicate that *the*

(14) Servis, K. L.; Shue, F.-F. *J. Am. Chem. Soc.* **1980**, *102*, 7233.

(15) (a) Singh, G.; Wolfsberg, M. *J. Chem. Phys.* **1975**, *62*, 4165. (b) Skaron, S. A.; Wolfsberg, M. *J. Am. Chem. Soc.* **1977**, *99*, 5253.

Table IV. Predicted ^2H Isotopic Conformer Populations^a

sites of ^2H	method of analysis	
	QUIVER ^b (K_{eq})	composite ^c (K_{eq})
1d	(1.151 5)	
8	0.090 66	
9	0.085 82	
10	0.090 09	
11	0.087 90	
12	0.090 09	
13	0.090 66	
14	0.097 26	
15	0.058 12	
16	0.075 70	
17	0.077 62	
18	0.096 93	
19	0.059 17	
1e	(1.174 6)	(1.175 5)
1f	(1.191 6)	(1.200 7)
1g	(1.352 5)	(1.353 5)
8, 9	0.093 75	0.093 74
9, 10	0.093 07	0.093 15
8, 10	0.098 35	0.098 41
11, 12	0.095 41	0.095 41
12, 13	0.098 39	0.098 40
11, 13	0.095 96	0.096 01
14, 15	0.068 09	0.068 10
15, 16	0.053 96	0.053 00
14, 16	0.087 87	0.088 70
17, 18	0.089 86	0.090 65
18, 19	0.069 11	0.069 10
17, 19	0.056 18	0.055 33
1h	(1.326 0)	1.326 0)
8, 11	0.063 44	0.063 44
9, 11	0.060 05	0.060 05
10, 11	0.063 05	0.063 04
8, 12	0.065 01	0.065 02
9, 12	0.061 55	0.061 55
10, 12	0.064 61	0.064 61
8, 13	0.065 43	0.065 43
9, 13	0.061 93	0.061 93
10, 13	0.065 01	0.065 02
14, 17	0.060 11	0.060 10
15, 17	0.035 91	0.035 91
16, 17	0.046 77	0.046 77
14, 18	0.075 05	0.075 05
15, 18	0.044 84	0.044 85
16, 18	0.058 41	0.058 41
14, 19	0.045 81	0.045 81
15, 19	0.027 37	0.027 37
16, 19	0.035 65	0.035 65
1i	(1.399 6)	(1.411 3)
1j	(1.611 7)	(1.625 1)
8, 9, 10	0.304 70	0.305 84
11, 12, 13	0.312 41	0.313 23
14, 15, 16	0.187 82	0.186 69
17, 18, 19	0.195 07	0.194 24
1k	(1.557 4)	(1.558 7)
1l	(1.855 8)	(1.871 5)
1m	(1.829 3)	(1.832 3)
1n	(2.179 8)	(2.000 2)

^a $T = 162.55$ K. ^b Calculated with QUIVER. ^c Calculated as a composite of reduced isotopic partition function ratios (obtained from QUIVER) of isotopic conformers of isotopomer **1d**.

deuterium isotope effect on conformational preference is, by far, the major factor in observed nonadditive equilibrium isotope effects in this ion.

(16) Only chemical shift differences, δ , are predicted theoretically. For ease of comparison, the relative intensities of peaks in the theoretically predicted spectra are drawn proportional to those observed experimentally (with the exception of peaks corresponding to isotopomers with degenerate 1,2 hydride shifts).

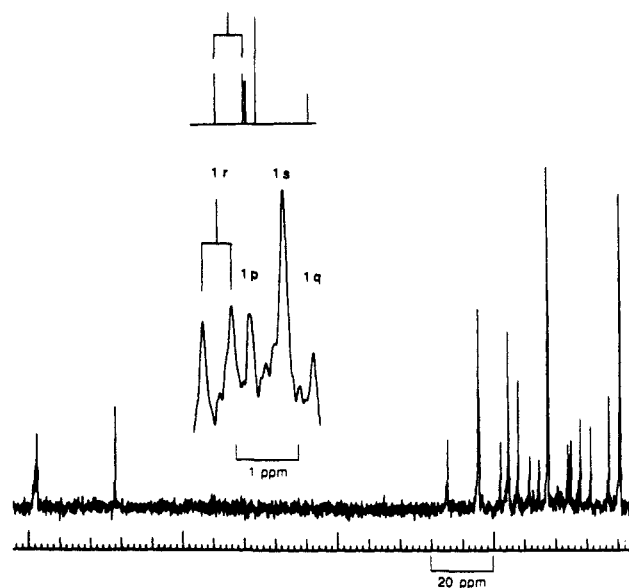


Figure 4. Proton-decoupled ^{13}C NMR spectra, centered at $\delta \sim 100$, of a scrambled sample of the $^{13}\text{C}_2$ -2,3-dimethyl-2-butyl cation in $\text{SbF}_5/\text{SO}_2\text{ClF}$ at -56 $^\circ\text{C}$. Inset: Expansion of downfield region ($\delta \sim 198$ – 200) of averaged cation/methine C resonances of natural-abundance mono- and dilabeled ^{13}C isotopomers of the 2,3-dimethyl-2-butyl cation in $\text{SbF}_5/\text{SO}_2\text{ClF}$ at -97 $^\circ\text{C}$. Upper trace of inset: spectra predicted by QUIVER.

^{13}C Equilibrium Isotope Effects

When precursor labeled with two ^{13}C methyl groups was ionized, two methyl peaks were seen in the ^{13}C NMR in a ratio of $\sim 2:1$. As might be expected, the methyls scrambled before the sample could be observed. This presumably occurs through the reversible rearrangement to the (secondary) 3,3-dimethyl-2-butyl cation. However, the methyl interchange process is slow on the NMR time scale and does not cause line broadening. From statistical considerations, the stronger upfield peak could be assigned to isotopomers (in rapid equilibrium) where the labeled methyls are attached to adjacent carbons, **1v** (Chart II), and the weaker downfield peak to isotopomers, **1t**, where the labeled methyls are attached to the same carbon. The temperature-dependent splitting between these peaks is the result of an equilibrium isotope effect (secondary), where ^{13}C methyl is favored next to C^+ . Warming the sample led to an equilibrium mixture of the three isomeric tertiary hexyl cations and eventually produced further scrambling that yielded a mixture of all possible dilabeled ^{13}C isotopomers of the $^{13}\text{C}_2$ -2,3-dimethyl-2-butyl cation. The downfield region (inset, Figure 4) now consisted of peaks corresponding to the nonsymmetrically labeled isotopomers with equilibria shifted by the primary equilibrium isotope effect and combinations of primary and secondary equilibrium isotope effects. Peak assignments followed from comparison of spectra obtained prior to and during scrambling, earlier literature,^{2c,17} and theoretical evaluation of the equilibrium isotope effect.

Prior to scrambling, only a small peak due to naturally abundant ^{13}C for the cation/methine carbon (**1p**) was evident in the downfield region. During the scrambling process, stronger peaks resulting from rearrangement of the enriched carbons of the dilabeled ion were seen to grow in. Downfield of the natural-abundance peak, a doublet due to spin-spin coupling ($^1J_{\text{CC}} = 29.9$ Hz) appeared, while upfield of the natural-abundance peak, two singlets appeared. The doublet could be assigned to the dilabeled isotopomer, **1r**, with two ^{13}C directly bonded (the labeled methyl carbon adjacent to the labeled inner carbon). The chemical shift difference between the peak lying furthest upfield in the spectrum following scrambling and the peak of the naturally abundant isotopomer, **1p**, is nearly exactly that seen earlier with the, spe-

(17) Krishnamurthy, V. V.; Prakash, G. K. S.; Iyer, P. S.; Olah, G. A. J. *Am. Chem. Soc.* **1985**, *107*, 5015.

Table V. Experimental and Theoretical ^{13}C Equilibrium Isotope Effects for Isotopomers **1p** and **1r-t^e**

	temp (K)	K_{eq}		δ (Hz)	
		exptl ^b	calcd ^c	exptl ^d	calcd ^e
1p	164.75	1.0163	1.0162	69.890	69.719
	172.55	1.0152	1.0154	65.513	66.031
	175.95	1.0153	1.0150	65.745	64.522
	184.05	1.0137	1.0142	59.000	61.141
	192.45	1.0135	1.0135	58.325	57.918
	207.35	1.0123	1.0123	52.827	52.796
	211.15	1.0121	1.0120	52.155	51.595
	212.45	1.0117	1.0119	50.436	51.193
	ΔH^f	6.3 ± 0.4	6.2		
	1r	164.75	1.0252	1.0195	107.867
172.55		1.0239	1.0184	102.446	79.020
175.95		1.0228	1.0180	97.852	77.143
184.05		1.0213	1.0170	91.437	72.932
192.45		1.0205	1.0160	88.114	68.915
207.35		1.0187	1.0145	80.285	62.528
211.15		1.0182	1.0142	78.195	61.031
212.45		1.0176	1.0141	75.591	60.530
ΔH		10.3 ± 0.4	7.8		
1s		164.75	1.0074	1.0131	31.748
	172.55	1.0073	1.0125	31.562	53.736
	175.95	1.0067	1.0122	29.097	52.582
	184.05	1.0064	1.0116	27.513	50.000
	192.45	1.0065	1.0110	28.231	47.543
	207.35	1.0062	1.0101	25.850	43.637
	211.15	1.0060	1.0099	25.693	42.720
	212.45	1.0059	1.0098	25.288	42.413
	ΔH	2.0 ± 0.3	4.8		
	1t	164.75	1.0198	1.0062	7.082
		1.0188		6.717	
167.65		1.0188	1.0061	6.711	2.197
170.25		1.0188	1.0059	6.713	2.125
173.65		1.0194	1.0058	6.945	2.089
174.75		1.0171	1.0057	6.108	2.053
177.05		1.0154	1.0056	5.507	2.017
180.55		1.0170	1.0054	6.095	1.945
185.25		1.0136	1.0052	4.883	1.874
186.45		1.0136	1.0052	4.880	1.874
187.55		1.0128	1.0051	4.584	1.838
197.25		1.0119	1.0047	4.271	1.694
208.55		1.0119	1.0043	4.268	1.550
213.75		1.0127	1.0041	4.570	1.478
ΔH	12.0 ± 1.6	3.0			

^a Refer to Chart II. ^b Evaluated as $(\Delta + 2\delta)/(\Delta - 2\delta)$; δ for isotopomers **1p**, **1r**, and **1s** were measured for equilibrating cation/methine carbons, $\Delta = 276$ ppm. δ for isotopomer **1t** was measured for equilibrating methyl carbons, $\Delta = 23$ ppm. ^c Equilibrium isotope effect calculated with QUIVER. ^d δ recorded at 62.8 MHz. ^e δ calculated for 62.8 MHz; for isotopomers **1p**, **1r**, and **1s** were calculated for equilibrating cation/methine carbons, $\Delta = 276$ ppm. δ for isotopomers **1t** and **1u** were calculated for equilibrating methyl carbons, $\Delta = 23$ ppm. ^f Units: cal/mol.

cifically synthesized, symmetrically dilabeled isotopomer, **1q** which has $K_{\text{eq}} = 1.0$,^{2e} and the peak is, therefore, assigned to this isotopomer. The remaining peak is assigned to the isotopomer, **1s**, with a ^{13}C methyl on the carbon away from the labeled inner carbon.

The downfield multiplet of peaks (inset, Figure 4) provides data from which to simultaneously obtain the primary equilibrium isotope effect and combinations of primary and secondary equilibrium isotope effects. These are collected in Table V together with theoretically determined values. The values for the equilibrium isotope effects in isotopomer **1p**^{2e} and **1r**¹⁷ are almost exactly the same as those obtained earlier. The observation of the doublet, due to spin-spin coupling, downfield of the naturally abundant isotopomer indicates that the secondary equilibrium isotope effect is in the same direction as the primary equilibrium isotope effect. Thus, ^{13}C prefers to be at the cationic center rather than at the methine position or on a methyl attached to the cationic

Table VI. Predicted ^{13}C Isotopic Conformer Populations at 164.75 K

site of ^{13}C	method of analysis		
	QUIVER ^a (K_{eq})	composite ^b (K_{eq})	
1p	(1.016 2)		
	1	0.504 02	
	2	0.495 98	
1r	(1.019 5)	(1.019 3)	
	1, 5	0.252 41	0.252 39
	1, 6	0.252 41	0.252 39
	2, 3	0.244 69	0.244 75
	2, 4	0.250 49	0.250 49
1s	(1.013 1)	(1.013 1)	
	1, 3	0.248 71	0.248 71
	1, 4	0.254 55	0.254 55
	2, 5	0.248 37	0.248 37
	2, 6	0.248 37	0.248 37
1t	(1.006 2)	(1.006 2)	
	3, 4	0.498 45	0.498 45
	5, 6	0.501 56	0.501 55
1u	(1.003 0)		
	3	0.246 72	
	4	0.252 52	
	5	0.250 38	
	6	0.250 38	

^a Calculated with QUIVER. ^b Calculated as a composite of reduced isotopic partition function ratios obtained from QUIVER of isotopic conformers of isotopomer **1p** and **1u**.

center rather than away from it. The equilibrium constant for the secondary isotope effect can be obtained from the measurements on the isotopomers where primary and secondary isotope effects combine in both directions and from the equilibrium constant for the primary effect. It is found to be about half the value of the primary isotope effect. The agreement between experimentally and theoretically determined values for the primary ^{13}C equilibrium isotope effect is good. Although theoretically determined values underestimate the contribution of the secondary equilibrium isotope effect, the overall agreement between theory and experiment is still quite good.

The question arises as to nonadditivity of ^{13}C equilibrium isotope effects. The small differences in the equilibrium populations of the label in the isopropyl carbons of the monosubstituted isotopomer, **1u** (Table VI), suggest that the isotopomer with two ^{13}C methyls on the same side, **1t**, should have an isotope effect slightly greater than the square of that for one ^{13}C methyl. The calculations, both from the full theoretical treatment and from the product of the $(s_2/s_1)^f$'s of the monosubstituted isotopomer **1u**, do support this expectation. Experimentally, we could not detect any conformational nonadditivity, as this would require accurately measuring the chemical shifts of the monolabeled and the symmetrically and unsymmetrically dilabeled isotopomers with ^{13}C only on the methyls. The effect of nonadditive ^{13}C isotope effects for the methyl C's is calculated to increase $\delta < 0.003$ ppm (0.2 Hz at 62.8 MHz) at the lower temperature limits of our experiments ($T = 164.75$ K). Of course, the increase in δ would be larger by a factor of 10 for the cation/methine C's, but this would require extensive labeling of the cation and would provide little additional benefit to this study. The (almost) exact agreement in the predicted populations of isotopic conformers calculated by the two methods shows that there is little if any cooperative interaction on vibrational frequencies for multiple ^{13}C substitution, with the exception of isotopomer **1r** with directly bonded ^{13}C .

Conclusions

The experimental method of observing mixtures of isotopomers allowed us to obtain very accurate data on relative equilibrium isotope effects in cases of multiple isotopic substitution. Theoretical calculations were able to model these effects quite well. The predicted secondary deuterium and ^{13}C equilibrium isotope effects closely reflect hyperconjugative distortion of the C-H and C-C bonds and the associated force constants. The considerable

nonadditivity in the isotope effect seen in the multiply deuterated ions is found to be largely due to perturbation of conformational populations. Nonconformational nonadditivity was found to be relatively minor.

In this ion, the isotopic conformational preference, which led to the considerable nonadditivity, was predictable because of the expected strong dependence of hyperconjugation on overlap. However, in other cases, the observation of substantial nonadditivity on multiple isotopic substitution might be a novel and valuable indication of conformational preference. This concept is related to the isotopic perturbation method for detecting rapid equilibrium reactions but uses differences in isotope effect at different positions in place of the differences in chemical shift employed in the conventional isotopic perturbation method.

The remaining disagreement between theory and experiment may result from the need for higher level quantum mechanics calculations for frequency analyses, as the level of calculations may not be high enough to reproduce features of hyperconjugative distortion of the C-H and C-C bonds within the real ion accurately enough. The energy surface involving torsion around single bonds may be quite flat, and small changes in the dihedral angle (evident in differences of structures in going from 3-21G to 6-31G* geometry optimizations) may result in significant changes in the predicted equilibrium isotope effects. The force field involving the motion of the center two carbons, and thus the calculated primary ^{13}C equilibrium isotope effect, does not seem as likely to be as sensitive to small changes in geometry.

Experimental Section

d -[^{13}C]-2,3-Dimethyl-2-butanol (~50% Deuteration in Two Methyl Groups). A two-neck 100-mL round-bottom flask was charged with barium carbonate (10 g, 5.1×10^{-2} mol, 90% ^{13}C enriched; Mound Laboratories) and evacuated on a vacuum line. Isopropyl bromide Grignard reagent (5.1×10^{-2} mol) in diethyl ether was attached to the vacuum line by a short length of vacuum hose, frozen in liquid N_2 , and the flask was evacuated. After the ether solution was thawed and allowed to return to room temperature, sulfuric acid was added dropwise to the barium carbonate through the second neck of the flask, liberating ^{13}C -enriched carbon dioxide. Carbon dioxide uptake by the Grignard solution was facilitated by swirling. After 2 h, the ether solution was removed from the vacuum line, the product worked up with dilute sulfuric acid, and the ether removed by short-path distillation to yield [1- ^{13}C]isobutyric acid, 2.5 g (56%). ^{13}C NMR (CDCl_3): δ 182.3, 33.7 ($^1J(\text{H}-^{13}\text{C}) = 127.6$ Hz, $^1J(^{13}\text{C}-^{13}\text{C}) = 55.1$ Hz), 18.6.

Thionyl chloride (2.4 g) in benzene (5 mL) was added dropwise to [1- ^{13}C]isobutyric acid (1.5 g) in benzene (10 mL) and the resultant mixture refluxed for 1 h. After removal of excess thionyl chloride, ethanol (6 g) was added to the acid chloride solution and the mixture refluxed overnight. Fractional distillation followed by preparative gas chromatography (6-ft column SE-30 column, $T = 100$ °C) yielded [1- ^{13}C]ethyl isobutyrate: 1.0 g (50%). ^{13}C NMR: δ 176.5, 59.6, 33.6 ($^1J(\text{H}-^{13}\text{C}) = 127.6$ Hz, $^1J(^{13}\text{C}-^{13}\text{C}) = 55.1$ Hz), 18.5, 13.8.

[1- ^{13}C]Ethyl isobutyrate (0.4 g) was added to 2 equiv (1.2 g) of the methyl iodide Grignard reagent (~50% D) in diethyl ether. (Partially deuterated methyl iodide was prepared by deuterium exchange of the trimethyloxosulfonium iodide salt in 50:50 $\text{D}_2\text{O}/\text{H}_2\text{O}$ with a catalytic amount of potassium carbonate. Pyrolysis yielded deuterated methyl iodide and dimethyl sulfoxide.¹⁸) After workup and purification by

preparative gas chromatography (6-ft SE-30 column, $T = 80$ °C), [$^{13}\text{C}_2$]-2,3-dimethyl-2-butanol with 50% deuteration in the two methyl groups attached to C-OH was obtained; 0.24 g (60%). Percent deuteration was determined by ^1H NMR of both methyl iodide and 2,3-dimethyl-2-butanol. ^{13}C NMR: δ 74.8, 38.6 ($^1J(^{13}\text{C}-^{13}\text{C}) = 35.2$ Hz), 27.6 ($^1J(^{13}\text{C}-^{13}\text{C}) = 40.7$ Hz), 17.8.

d -2,3-Dimethyl-2-butanol (~50% Deuteration in Two Methyl Groups). This was synthesized as described above, except from ethyl isobutyrate (Aldrich) and methyl iodide Grignard reagent (~50% D).

d -2,3-Dimethyl-2-butanol (~50% Deuteration in One Methyl Group). This was synthesized as described above, except from 3-methyl-2-butanone (Aldrich) and methyl iodide Grignard reagent (~50% D).

[$^{13}\text{C}_2$]-2,3-Dimethyl-2-butanol. This was synthesized as described above, except from ethyl isobutyrate (Aldrich) and [^{13}C]methyl iodide (Aldrich).

Cation Sample Preparation. Cation samples were prepared by ionization of the corresponding alcohol with the molecular beam apparatus as previously described.¹⁹ Antimony pentafluoride (0.2–0.3 mL) and the alcohol (0.05–0.10 mL) were codistilled into an evacuated, glass chamber cooled in liquid nitrogen. The solvent (1.2 mL, total), sulfuric chloride fluoride, was distilled into the chamber prior to and following the codistillation of antimony pentafluoride and the alcohol. The method used achieves intimate mixing of reagents and suppresses rearrangement or polymerization of the cation sample to yield a clean cation preparation at a concentration suitable for NMR analyses. The frozen mixture was thawed slowly in a methanol/ethanol slush bath (–110 °C) and poured into attached NMR tubes with all glassware contacting the cation solution kept cold (–110 °C). The tubes were sealed and immediately frozen in liquid nitrogen until needed.

NMR Spectra. ^{13}C NMR spectra were recorded on a Bruker WM-250 at 62.8 MHz. Cation samples were placed in a precooled NMR probe following temperature calibration with 2-chlorobutane.²⁰ Spectra were recorded from –110 to –55 °C. Peak positions were referenced to external TMS in acetone- d_6 . Spectrometer acquisition parameters were tailored according to the demands of the experiment. Quadrature detection was used in all instances, and the center frequency was positioned at δ 32 when equilibrium isotope effects from the splitting of the upfield methyl carbons were analyzed and at δ 198 when the downfield cation/methine peaks were used. For the evaluation of the ^{13}C equilibrium isotope effects from analysis of the upfield peaks, 250 scans with a 20° pulse and digital resolution of 0.3 Hz/point (spectra width (SW) of 2500 Hz and a block size (SI) of 16K) were collected at each temperature. ^{13}C equilibrium isotope effects were evaluated from analysis of the downfield peaks by accumulating 4000 scans with a 20° pulse and a digital resolution of 0.6 Hz/point (SW 5000 Hz, SI 16K). Deuterium equilibrium isotope effects were evaluated from analysis of the downfield peaks by accumulating 256 scans (16 000 scans for the normal-abundance ^{13}C cation) with a 75° pulse width and a digital resolution of 1.9 Hz/point (SW 15151 Hz, SI 16K).

Acknowledgment. This work was supported by a grant from the National Science Foundation.

Registry No. ^{13}C , 14762-74-4; 2,3-dimethyl-2-butyl cation, 17603-18-8; deuterium, 7782-39-0.

(18) Cotton, F. A.; Fassnacht, J. H.; Horrocks, W. D., Jr.; Nelson, N. A. *J. Chem. Soc.* **1959**, 4138.

(19) Saunders, M.; Cox, D.; Lloyd, J. R. *J. Am. Chem. Soc.* **1979**, *101*, 6656.

(20) Kates, M. R. Ph.D. Thesis, Yale University, 1978.